

Transformer fault detection based on Raman analysis of the transformer oil (A case study)

M. Kadlečíková¹, J. Breza¹, J. Raditschová¹, E. Vančo², B. Butvinová³

¹ Faculty of Electrical Engineering and Information Technology, Slovak University of Technology in Bratislava, Ilkovičova 3, 812 19 Bratislava, Slovakia

² Centre for Nanodiagnosics, Slovak University of Technology in Bratislava, Vazovova 5, 812 43 Bratislava, Slovakia

³ Institute of Physics, Slovak Academy of Sciences, Dúbravská cesta 9, 845 11 Bratislava, Slovakia
E-mail: magdalena.kadlecikova@stuba.sk

Abstract

The paper reports on an experiment in the academic laboratory that aimed to detect a transformer fault by Raman spectroscopy of the transformer oil. Indicators of oil degradation (*eg* gases, sludge, cellulose) could not be detected. Combustion indicators (soot – graphitic particles, graphene particles, amorphous carbon) in the transformer oil were reliably detected by Raman measurements. The transformer was disassembled at the factory. It was shown that the magnetic core and electrical circuit of the transformer were irreversibly damaged and the contamination of the active parts of the transformer and the oil was massive. Two interturn short circuits were detected. It was confirmed that in the place of the coil shorts, where an electric arc burned, melting occurred of the winding conductors and of a part of the transformer core. Raman spectroscopy proved to be a useful method for rapid diagnostics of the events in a hermetically sealed transformer vessel.

INTRODUCTION

Basic data on the accident

The fault on the transformer was manifested by an alarm from the digital protection system. At the time of the fault, the transformer had been in operation for 3.5 years. When looking at the transformer body from outside, no deformation or destruction of the transformer vessel was visible. There were no signs of oil leakage or other defects (such as bulging) on the welds or other parts of the vessel. There was no visible change in paint color as a manifestation of long-term elevated temperature, oxidation of metal parts due to ambient humidity or melting at the terminal and cable interface, color marks (color patterns) revealing overheating of joints due to assembly errors, and no signs of damage (blackening) of terminals or bushings on the LV and HV sides of the transformer cover (Fig. 1).

EXPERIMENT

Raman spectroscopy

Raman spectroscopy is an optical method based on laser beam interaction with the analyte molecules. The excitation light is a laser beam with wavelength λ and wave number ν_0 . After interaction of the primary laser light with the substance most of the scattered radiation has the same frequency as the excitation beam, this is the so-called Rayleigh elastic scattering. In addition, the Raman spectrum contains longer and shorter wavelengths. The difference $\Delta\nu = |\nu_0 - \nu|$ is referred to

as the Raman shift. Its values are typical for particular substances. The Raman spectrometer Dilor-Jobin Yvon-Spex, type LabRam 300 with confocal micro-

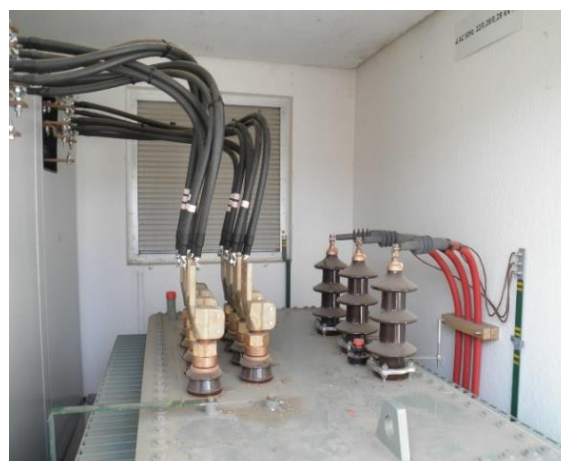


Fig. 1: LV and HV terminals and bushings on the oil transformer cover. The transformer was installed in the transformer part of a kiosk transformer station in a photovoltaic power plant. It is a three-phase oil transformer with a rated output of 1250 kVA for a nominal high voltage of 22 kV and 2×280 V low voltage. The three windings are Dyn1yn1 connected (delta connection on the higher voltage side, star connection on the lower voltage side, the clock angle is 1). The system is hermetically sealed in a radiator vessel and filled with a cooling and insulating medium – mineral oil. The container is naturally cooled by air. The winding materials are Cu and Al.

scope Olympus BX-40 is equipped with a He-Ne laser ($\lambda = 632.8 \text{ nm}$).

Prior to measurements, the spectrometer was calibrated to the dominant band of single crystalline (100)-oriented silicon at a wave number of 520.7 cm^{-1} . The secondary radiation was resolved with a 1800 grooves/mm grid monochromator and detected by a CCD multichannel air cooled detector. The monochromator slit and confocal slit were opened to maximum, $200 \text{ }\mu\text{m}$ and $1000 \text{ }\mu\text{m}$, respectively. The analysis was performed at room temperature, in the wavenumber range from 200 to 3000 cm^{-1} , the laser power was 5 mW , and $10\times$ (cuvette) and $100\times$ (watch glass) objectives were used. The total time of recording one spectrum from one point on the sample was approx. 100 seconds.

We took an oil sample from the encapsulated transformer and analyzed it in a quartz cuvette and dropwise on a watch glass. In the oil sample taken, filled into a narrow cuvette, only the Raman bands at $\approx 1440 \text{ cm}^{-1}$ and $\approx 1488 \text{ cm}^{-1}$ were recorded. Spectral analysis of the observed bands is not possible because the composition of the insulating oil is uncertain at this stage of its degradation. The Raman bands of the analyzed oil sample lie on a wide photoluminescence background, which points at the presence of impurities that contribute to luminescence. The Raman spectrum (Fig. 2), in the spectral range from 1200 to 1700 cm^{-1} are typical for carbon materials. We identified carbon black in the Raman spectrum of contaminated oil. Raman spectroscopy carbon black has been described in detail in [1]. Soot, is technically defined as the black solid product of incomplete combustion or pyrolysis of materials. Soot is primarily composed of carbon ($> 80\%$) and consists of agglomerated primary particles with diameters on the order of 10 to 30 nm comprising crystalline and amorphous domains.

The Raman spectrum of oil droplets is dominated by two bands. The first one is called a defective band D, centered at approx. 1316 cm^{-1} . The second band is called the G band and with its center between 1550 and 1650 cm^{-1} identifies graphite in the carbon material, hence the presence of sp^2 bound carbon atoms. For the sake of completeness, crystalline (ordered) graphite exhibits a Raman G band of Lorentzian shape at a wavenumber of 1580 cm^{-1} and at the same time an asymmetrical G' band at approx. 2700 cm^{-1} . The wide Raman band G centered between 1550 and 1650 cm^{-1} and the wide G' band centered at approx. 2650 cm^{-1} , as in our case (Fig. 3), indicates the presence of disordered graphite [2, 3]. Consistent with the results reported in [1], we observe a G band with a peak at approximately 1571 cm^{-1} and a FWHM of $\approx 100 \text{ cm}^{-1}$. The existence of the broad G band and simultaneously of the D band in the Raman spectrum gives evidence of defects in the crystal lattice of graphite and of the presence of different carbon sp^2 and sp^3 bound clusters.

The interpretation of the D and D' bands is more complicated. The D band is built by perturbations at the level of ≈ 2 to 5 nm in crystalline graphite or graphene structures [2]. The Raman spectrum of contaminated transformer oil shows a D' band with a center at approx. 1604 cm^{-1} , which can be induced by defects in graphite crystals but also the result of heat treatment of hydrocarbons, when the D' band is observed at approx. 1620 cm^{-1} [1].

The bands D, D' and G are mutually related. The bands D, D' and G are partially overlapped. The use of the red He-Ne laser excitation results in a worse resolution of these spectral components. Due to the shape of the D band, the presence of an amorphous carbon phase can also be considered. Contaminated oil is a material containing most likely all kinds of carbon atom bonds (even sp^1), which is not exceptional in the burn. In the Raman spectrum, we identified carbon blacks composed of graphite, dis-ordered graphite, graphene, and amorphous carbon. Depending on the combusted material and combustion conditions, the carbon black differs in its aggregated morphology, particle size and nanostructure of the particles [4]. They contain carbon particles of the micro and nanoscales. Not surprisingly,

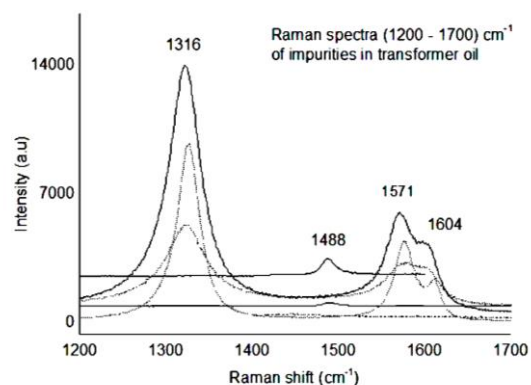


Fig. 2: Raman spectra of transformer oil and of the soot in wave number range from 1200 to 1700 cm^{-1}

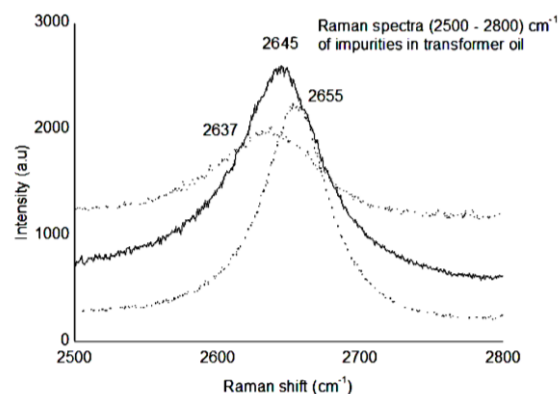


Fig. 3: Raman spectra of soot in wave number range from 2500 to 2800 cm^{-1}

the presence of nanocrystalline graphite and graphene was also confirmed in the degraded oil by Raman spectroscopy.

The final diagnosis of the transformer failure was confirmed by the image from the production plant where the transformer was disassembled.



Fig. 4: Transformer pulled out of the oil vessel. The electrical insulation system of the transformer consists of combined dielectrics: mineral oil and paper.

Diagnostics of the transformer fault

After removing the transformer body from the oil sump (Fig. 4), damage to the high-voltage coil was first observed (Figs. 5 to 7). Figure 7 shows a locally burned HV winding. After complete disassembly of the transformer, damage to the magnetic circuit of the transformer (Fig. 8) and extensive destruction of the low-voltage coil (Figs. 9 to 12) were also found.

According to the appearance of the destruction of the transformer winding, the evolution of the event before the transformer failure was terminated by breaking the coil insulation of the winding and transitioning to an interturn short circuit. After the destruction of the winding insulation, the first coil short circuit probably occurred precisely in the part of the HV winding visible in Fig. 7.

The interturn short circuit current passes through an arc between the coil conductors. The temperature reaches and exceeds the melting point of the conductor metal. Thus the electric arc burning at the interturn short circuit led to the melting of the winding conductor (melting point of aluminum is 660 °C, the melting point of copper is 1083 °C). The molten material of the LV coil winding can be seen mainly in Fig. 12.

The burning electric arc in the LV coil near the transformer core (Fig. 8) was boosted up by the aluminum present, which reduced iron oxides and gave rise to liquid iron. At temperatures above 768 °C, iron loses its ferromagnetic properties. The melting of a portion of the transformer core is shown in the



Fig. 5: Damaged HV coil visible after removing the transformer from the oil sump. The fault on the HV winding is located approximately in the middle of the column.



Fig. 6: Detail of the insulation of the HV coil of the transformer

photograph. Iron (Fe) has a melting point of 1528 °C and the transformer sheet used does not have a significantly different melting point from pure iron. It is obvious that local and short-term temperature at the level of the melting point of iron was reached in the arc, which damaged the transformer core.



Fig. 7: Exposed damaged winding of the transformer HV coil. The short circuit is located about 50 degrees from the busbar. The combustion plant has an irregular shape and a range from the surface to the first cooling channel.

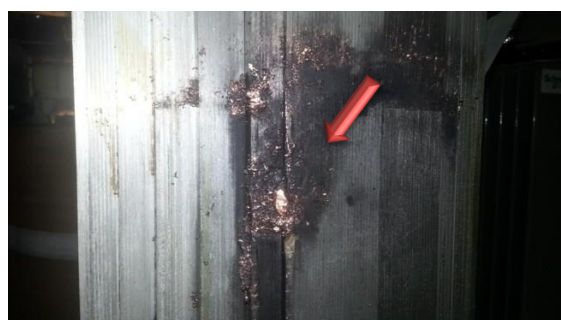


Fig. 8: Arrows indicate the melting of the transformer's magnetic core.



Fig. 9: LV coil foil winding. The short occurred at the top of the LV coil about 80 degrees to the right of the LV busbar. The destruction leads from the first layer of Cu conductors to the ninth. (It is possible that a developing fault in the HV winding has affected this adjacent LV winding.)



Fig. 10: Detail of the location of the interturn short circuit on the LV coil of the transformer. The interturn short went through 9 layers of the winding.

An interturn short in the transformer winding is dangerous because it results in only a small increase of the current in the winding but in a sharp multiple increase of the current in the short circuit, and locally high temperatures are reached which the cooling

medium is unable to drain the heat. Thermal energy is consumed for local heating (up to the boiling point) and evaporation of the oil, which rises to the surface and, in addition, it is ionized and becomes conductive. In the cooling medium (Fig. 13) there are visible residues after burning, which may be the metal itself, fragments of burnt insulation or oil fraction formed by local boiling of the cooling medium in contact with the molten metal.



Fig. 11: Combustion site at the point of short circuit, where an electric arc has formed, which has led to deterioration of the insulation and melting of the winding conductor.



Fig. 12: Detail of the molten winding of the LV transformer coil.

CONCLUSION

There may be several causes of two interturn short circuits, each of which, even individually, can malfunction the transformer. Without external manifestations, gradual degradation of the winding



Fig. 13: Transformer oil degradation. Fresh oil (according to the manufacturer's characteristics) is pale yellow and transparent.

insulation of the HV coil transformer coils could take place, which could be caused, for example, by insulation wetting [5] or by local overheating due to insufficient heat dissipation at this location. This condition led to reduction in the insulating strength of the interturn insulation. However, the causes of insulation damage may be different, *eg* a hidden insulation defect – local weakening of the insulation caused during production, shape deformation of the conductor surface in this place, or a small metal cut, a tip on the winding that pierces the insulation during vibrations. All these circumstances can lead to a local increase in losses, subsequent degradation of the insulation and, after some time, to an electrical breakdown. Short circuit insulation can also cause a short circuit of the HV or LV coil. (Overvoltage is any voltage that is higher than the highest nominal voltage (specified by the manufacturer on the nameplate). Overvoltage generally strains both conductors and insulation. Short circuits on one of the coils and subsequent propagation of the destruction to the other coil are more likely than independent interturn short-circuits. Probably due to effective shortcircuit protection, fire did not occur and the transformer in the PV plant did not burn completely.

At the beginning of this work was a research experiment in an academic laboratory, the aim of which was to detect a transformer failure based on the Raman spectrum of transformer oil. Indicators of oil degradation (*eg* gases dissolved in oil, sludge, cellulose) could not be detected. Combustion indicators (carbon blacks, graphitic particles, amorphous carbon) in transformer oil were reliably detected by Raman spectroscopy. Raman spectroscopy has been shown to be a useful alternative for diagnosing transformer faults. When used for this purpose, its important features are a short analysis time (minutes), fast detection of carbon bonds and obtaining an initial view of the process taking place in a hermetically sealed transformer vessel.

ACKNOWLEDGEMENT

We are grateful to the scientific grant agency VEGA of the Ministry of Education, Science, Research and Sport of the Slovak Republic for financial support of project No. 1/0532/19 and to the Slovak Research and Development Agency, contract No. APVV-17-0169. We thank for providing photographs (Figs. 4 to 13) of the disassembled transformer.

REFERENCES

- [1] A. Sadezky, H. Muckenhuber, H. Grothe, R. Niessner and U. Poschl, "Raman microspectroscopy of soot and related carbonaceous materials: Spectral analysis and structural information", *Carbon*, vol. 43, pp. 1731–1742, July 2005.
- [2] C. Ferrari and J. Robertson, "Resonant Raman spectroscopy of disordered, amorphous, and diamondlike carbon", *Physical Review B*, vol. 64, 075414, August 2001.
- [3] C. Ferrari, "Raman spectroscopy of graphene and graphite: Disorder, electron-phonon coupling, doping and nonadiabatic effects", *Solid State Communications*, vol. 143, pp. 47–57, July 2007.
- [4] M. Singh and R. L. Vander Wal, "Nanostructure Quantification of Carbon Blacks", *Journal of Carbon Research, C*, vol. 5, pp. 2–12, December 2019.
- [5] I. Kolcunová, J. Kurimský, B. Dolník and M. Matviša, "Diagnostika distribučného transformátora v laboratórnych podmienkach", *Starnutie elektroizolačných systémov*, vol. 7, no. 1, pp. 20–25, 2012.